

Self-Supervised Graph Learning with Hyperbolic Embedding for Temporal Health Event Prediction

Chang Lu, Chandan K. Reddy, *Senior Member, IEEE*, Yue Ning

Abstract—Electronic Health Records (EHR) have been heavily used in modern healthcare systems for recording patients’ admission information to hospitals. Many data-driven approaches employ temporal features in EHR for predicting specific diseases, readmission times, or diagnoses of patients. However, most existing predictive models cannot fully utilize EHR data, due to an inherent lack of labels in supervised training for some temporal events. Moreover, it is hard for existing works to simultaneously provide generic and personalized interpretability. To address these challenges, we first propose a hyperbolic embedding method with information flow to pre-train medical code representations in a hierarchical structure. We incorporate these pre-trained representations into a graph neural network to detect disease complications, and design a multi-level attention method to compute the contributions of particular diseases and admissions, thus enhancing personalized interpretability. We present a new hierarchy-enhanced historical prediction proxy task in our self-supervised learning framework to fully utilize EHR data and exploit medical domain knowledge. We conduct a comprehensive set of experiments and case studies on widely used publicly available EHR datasets to verify the effectiveness of our model. The results demonstrate our model’s strengths in both predictive tasks and interpretable abilities.

Index Terms—Electronic health records (EHR), hyperbolic embeddings, graph learning, model interpretability

I. INTRODUCTION

GIVEN the wide potential of Electronic Health Records (EHR), mining interpretable predictive patterns from EHR data has significant impacts on healthcare and has drawn a lot of attention in recent years. EHR data are complex in nature and typically contain sequences of patients’ admission records, such as diagnoses, clinical notes, and medicines. Effective analysis of EHR data is important for both medical professionals and patients as it can provide preventative health alerts and personalized care plans.

A variety of predictive models using deep learning technology have been proposed for predicting temporal events, such as diagnosis prediction [1]–[4], mortality prediction [5]–[7], risk prediction [8]–[10], and medicine recommendation [11], [12]. A common supervised training approach to utilize EHR data for temporal event prediction is to use previous records as features and the records of next admissions as labels. However, this approach will inherently ignore patients’ final

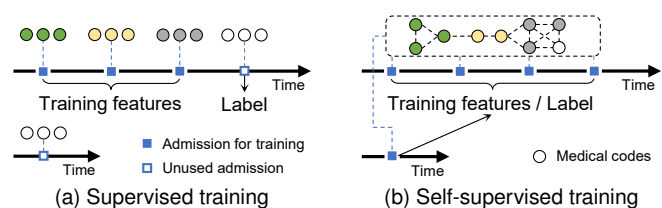


Fig. 1. An example of supervised training and self-supervised training for predicting temporal event using graph data.

admissions due to the lack of labels. Moreover, learning effective representations for medical concepts with the help of domain knowledge is still an open problem in healthcare applications. In summary, there are still some challenges for predictive models using temporal information of EHR data.

(i) *Fully utilizing EHR data.* A large number of EHR records are unused in traditional supervised training. Final admission records of patients, including single admissions, are discarded for training because the labels are missing for next potential admissions. Fig. 1(a) shows the reason for lacking labels while predicting temporal events. For multiple-admission patients (top arrow), the final admission record is used as the label for a prediction and cannot be used as training features. For single-admission patients (bottom arrow), there are no labels because there are no next admissions. However, according to the statistics of a widely used EHR dataset [13], the number of multiple-admission patients is only 20% of single-admission patients. Hence, a majority of valuable information in EHR data is discarded.

(ii) *Exploiting disease hierarchies during prediction.* In modern disease classification systems like ICD-9-CM [14], diseases are classified into various categories as medical codes in multiple levels and form a hierarchical structure. Existing works such as GRAM [3] and G-BERT [12] mainly use this structure to extract disease features by attention methods. However, this domain knowledge is helpful in guiding model predictions. By predicting disease hierarchies, representations of diseases can be further refined.

(iii) *Learning hidden representations for related disease.* Most existing works treat diseases independently, but neglecting the disease interactions, i.e., complications. However, such complications are generally crucial in medical practice. For example, longstanding hypertension will eventually lead to heart failure. Consequently, it is very common for patients with heart failure to have been suffering from hypertension prior to being admitted for a heart failure condition [15].

(iv) *Simultaneously providing generic and personalized*

C. Lu and Y. Ning are with the Department of Computer Science, Stevens Institute of Technology, New Jersey, NJ, 07310. E-mail: clu13@stevens.edu, yue.ning@stevens.edu

C.K. Reddy is with the Department of Computer Science, Virginia Tech, Arlington, VA 22203. E-mail: reddy@cs.vt.edu

This work has been submitted to the IEEE for possible publication. Copyright may be transferred without notice, after which this version may no longer be accessible.

interpretability. Generic interpretability provides discovered common knowledge such as disease complications from over-all patients’ records. Personalized interpretability refers to explanations for individual patients based on their personal admission records. However, current works [3], [4], [16], [17] mainly focus on one type of interpretability, while it is critical to simultaneously provide both generic and personalized interpretability.

To address these challenges, we propose **Sherbet**, a *self-supervised graph learning framework with hyperbolic embeddings for temporal health event prediction*. As a subset of unsupervised learning methods, the self-supervised learning method in this work is different from other pre-training methods, such as G-BERT [12]. We design a special proxy task for self-supervised learning to hierarchically predict historical diagnoses of patients. Fig. 1(b) shows in general how self-supervised learning fully uses EHR data. The proxy task constructs an interaction graph for medical codes in all admissions rather than treats each admission independently. It enables us to incorporate single-admission patients and the final admissions of multiple-admission patients by generating new labels for all admissions. When implementing this task, we first pre-train disease representations using a new hyperbolic embedding method with information flow to reconstruct the disease hierarchical structure. In order to model disease interactions, we next construct a weighted and directed graph for diseases based on their occurrences in patients’ admission records. Then we design a graph encoder architecture for self-supervised learning. The first part of the graph encoder is a graph neural network on the constructed graph to extract hidden disease representations and further learn the disease complications. Then, we develop a multi-level attention mechanism as the encoder to learn the representation of admissions and patients from the admission records. The contribution of specific diseases and admissions to a given prediction task can thus be quantified. The self-supervised learning component, which is also the decoder, is designed with the proxy task of hierarchically predicting historical diseases. Finally, we build a fine-tuning module for specific tasks. The main contributions of this work are summarized as follows:

- We propose a novel self-supervised graph learning framework and a hierarchy-enhanced historical prediction task to fully exploit the admission records in EHR data and hierarchical structures of medical codes in predictions.
- We propose a new hyperbolic embedding method with an information flow strategy to pre-train medical code representations. It can simultaneously consider hierarchical domain knowledge and similarities among medical codes.
- We design a weighted and directed disease interaction graph to learn the disease complications. Together with a multi-level attention mechanism, the proposed model is able to provide generic and personalized interpretability.

The rest of this paper is organized as follows: Section II summarizes the related works. Section III introduces the formulation of the prediction problem and the self-supervised learning task. Then, we demonstrate the experimental settings, results, and discussions in Sections IV and V. Finally, we

summarize our work in Section VI and discuss the potential future research.

II. RELATED WORKS

Predictive Models in Healthcare: Deep learning methods have been widely adopted for learning effective representations of complex and dynamic data in a wide range of applications including temporal event modeling in the healthcare domain. Choi *et al.* [1] proposed DoctorAI to predict diagnoses in the next admissions and the time interval of hospital readmissions using recurrent neural networks (RNN) with GRU [18] cells. A reverse-time RNN with an attention model, RETAIN, is proposed by Choi *et al.* [16] to predict heart failure and provide some interpretability of predictive models. Nguyen *et al.* [8] proposed DeepR which regards the diseases as words and the admission records as sentences and uses convolutional neural networks (CNN) as a language model to predict re-admission possibilities of patients in the next three months. Ma *et al.* [17] proposed Dipole using a bi-directional RNN along with various attention mechanisms to predict diagnoses of patients’ next admissions. Bai *et al.* [4] consider the time duration between two admissions and propose the Timeline model. However, as discussed above, these predictive models usually do not consider data that do not have labels (such as single and last admissions) and thus cannot fully utilize the potential of EHR data.

Unsupervised and Self-supervised Learning in Healthcare: Self-supervised learning refers to training models with automatically generated labels [19]. It is used for obtaining distinguishable features of samples by pre-training the model on proxy tasks. Gidaris *et al.* [20] created a pretext task to predict image rotation using ConvNet. Chen *et al.* [21] used context restoration, which is also a self-supervised learning strategy for medical image analysis. A common approach when using EHR data is to treat the diseases and the admission records as words and sentences, respectively. Then popular language models such as Transformer [22] and BERT [23] can be applied to learn the representation of diseases. Choi *et al.* [3] applied GloVe [24] to initialize disease embeddings in a medical ontology tree using labeled data. Shang *et al.* [12] proposed the G-BERT model to recommend medicines for patients considering an admission as a sentence and using BERT to pre-train disease embeddings. However, one problem of applying language models on EHR data is that diagnoses in an admission record typically do not have an ordering (like words in a sentence). Therefore, language models may not fit EHR data well because a different order of diagnoses may lead to significantly different prediction results.

Graph Neural Networks: Recently, graph neural networks have become popular and effective to model EHR data. Kipf *et al.* proposed a graph convolutional neural network [25] to generalize convolutional neural networks to handle graph-structured data. Choi *et al.* [3] used a medical ontology graph based on hierarchical domain knowledge and applied an attention mechanism to aggregate disease embeddings in different hierarchies. Shang *et al.* [12] also utilized this knowledge but designed a two-stage attention method for diseases. Choi *et*

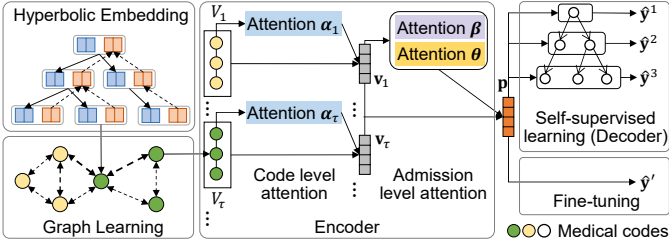


Fig. 2. An overview of the proposed Sherbet model. Hyperbolic representations of medical codes are firstly pre-trained with a hierarchical structure. Then, the Sherbet graph is constructed based on the occurrence of medical codes in admission records. A graph neural network is adopted to learn the hidden embedding of medical codes. Next, an encoder including the code level attention and admission attention is designed to encode the admission records of a patient into a patient vector. For the self-supervised learning, a historical hierarchy prediction task is designed to utilize the hierarchical structure of medical codes in prediction. Finally, after self-supervised learning, we can apply fine-tuning for specific prediction tasks.

al. [26] proposed GCT, a graph convolutional transformer by constructing a graph of diagnoses, treatments, and lab results. These models treat diseases independently, and do not take into account a common fact that diseases in different classes can also have strong interactions, i.e., disease complications. Moreover, the discussed methods only apply graph domain knowledge (e.g., hierarchical medical code classification) in feature extractions.

Given these problems in existing works, we develop a method that can utilize more information in EHR data. The proposed method takes disease hierarchical structures and hidden disease relations into account in temporal predictions. In addition, we also focus on providing interpretability at both disease and patient aspects.

III. THE PROPOSED METHODOLOGY

We first describe the basic notations and formulate the problem of predicting temporal events (Section III-A). Next, we demonstrate an unsupervised learning method to initialize disease representations using hyperbolic embeddings for the disease hierarchical structure (Section III-B). Then we introduce the strategy to construct the disease graph (Section III-C), followed by the proposed self-supervised learning method using a graph encoder-decoder (Section III-D). The fine-tuning of the model is performed after self-supervised learning (Section III-E). Finally, we discuss the interpretability of Sherbet from three different perspectives including the disease complications and specific contributions of historical diagnoses and admissions to the predictions (Section III-F). An overview of the system framework of the proposed Sherbet is shown in Fig. 2.

A. Problem Formulation

An EHR dataset contains temporal admission records of patients. In each admission, a patient is diagnosed with one or more diseases represented by medical codes, in the format of ICD-9-CM [14] or ICD-10 [27]. We denote the entire set of medical codes by $\mathcal{C} = \{c_1, c_2, \dots, c_{|\mathcal{C}|}\}$ in the EHR dataset. For a patient u , one clinical record $V_\tau^u \subset \mathcal{C}$ is a subset of

TABLE I
NOTATIONS USED IN THIS PAPER.

Notation	Description
\mathcal{D}	EHR dataset
\mathcal{H}, H	Disease hierarchical structure and level number
\mathcal{U}, \mathcal{C}	Sets of patients and medical codes
V_τ	τ -th admission record for a patient
\mathbf{E}	Embeddings of medical codes
\mathbf{X}	Learned hidden embeddings of medical codes
\mathbf{A}	Adjacency matrix of medical codes
\mathbf{v}_τ	Embedding vector of the τ -th admission
\mathbf{p}	Embedding vector of a patient

\mathcal{C} , where $\tau = 1, 2, \dots, T^u$ denotes the τ -th admission record of patient u who has a total of T^u admissions. In the rest of this paper, we drop the superscript u in V^u, T^u for better readability unless otherwise stated. The important symbols used in this paper are listed in Table I.

Definition 1 (EHR dataset). An EHR dataset is given by $\mathcal{D} = \{r_u | u \in \mathcal{U}\}$ where \mathcal{U} is the entire set of patients in \mathcal{D} , and $r_u = (V_1, V_2, \dots, V_T)$ is the admission records of patient u . Each admission $V_\tau \subset \mathcal{C}$ contains a subset of \mathcal{C} .

Definition 2 (Health Event Prediction). Given an EHR dataset \mathcal{D} and a patient u who has T historical admissions, the goal of the prediction task in this paper is to predict the future health event \mathbf{y}_{T+1} for patient u such as diagnosis or heart failure prediction. For instance, if the task is to predict the diagnoses for a patient's $(T+1)$ -th admission, the goal will be estimating the probabilities of all medical codes, i.e., $\mathbf{y}_{T+1} \in \{0, 1\}^{|\mathcal{C}|}$ in the $(T+1)$ -th admission of this patient.

B. Hyperbolic Embedding with Information Flow

The ICD-9-CM system provides a domain knowledge base to classify diseases into various categories represented by medical codes in multiple levels. In this system, the medical codes form a hierarchical structure \mathcal{H} with H levels, i.e., a tree. To obtain effective representations of medical codes, we aim to learn the embeddings of medical codes by reconstructing the skeleton of \mathcal{H} . We take advantage of the Poincaré ball model [28], [29] to learn the representations of the hierarchical structure, which encodes nodes in \mathcal{H} to a hyperbolic space. The distance in the hyperbolic space between embedding vectors \mathbf{e}_i and \mathbf{e}_j of two medical codes $c_i, c_j \in \mathcal{H}$ is defined as:

$$d(\mathbf{e}_i, \mathbf{e}_j) = \cosh^{-1} \left(1 + 2 \frac{\|\mathbf{e}_i - \mathbf{e}_j\|^2}{(1 - \|\mathbf{e}_i\|^2)(1 - \|\mathbf{e}_j\|^2)} \right). \quad (1)$$

In \mathcal{H} , higher level diseases can be regarded as a summary of their children, while lower level diseases provide more precise descriptions for their parents. Following this intuition, we also propose an information flow strategy to model the similarity and distinction among ancestor nodes and children nodes in \mathcal{H} . Together with the hyperbolic embedding, it is able to simultaneously consider the hierarchy and similarity of medical codes.

In practice, the medical codes recorded in EHR datasets are usually leaf nodes. In some cases when a patient is diagnosed

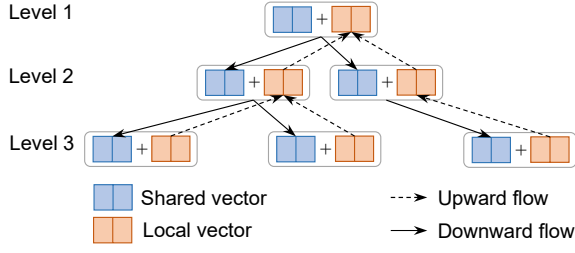


Fig. 3. Information flow in disease hierarchical structure

with higher-level diseases, i.e., non-leaf nodes, we recursively create virtual child nodes for each non-leaf node to pad them into virtual leaf nodes in the same level. Therefore, in this paper, the medical codes set \mathcal{C} contains only leaf nodes and virtual leaf nodes in the last level, and we use $|\mathcal{H}|$ to denote the total number of medical codes in \mathcal{H} . To represent the information flow in \mathcal{H} , we first assign each medical code c_i with two randomly initialized trainable embedding vectors, a shared vector $\mathbf{s}_i \in \mathbb{R}^d$ and a local vector $\mathbf{t}_i \in \mathbb{R}^d$. The shared vector \mathbf{s}_i is designed to represent the information inherited from its parent, i.e., similarity. The local vector \mathbf{t}_i is the private and more precise information of c_i that makes c_i different from its parent, i.e., distinction. Then, the public embedding vector \mathbf{e}'_i of c_i is calculated as

$$\mathbf{e}'_i = \lambda_i \times \mathbf{s}_i + (1 - \lambda_i) \times \mathbf{t}_i \in \mathbb{R}^d, \quad (2)$$

where λ_i is a trainable coefficient to integrate the shared and local vector. To capture the information flow in the disease hierarchical structure, we propose a hierarchical embedding method using the shared and local embedding vectors of each medical code. Fig. 3 shows the information flow in two directions, i.e., downward and upward flow. A downward flow indicates that the shared vector of a lower level medical code inherit the public vector of its parent, and an upward flow simulates the summary of this medical code's children by aggregating the children's local vectors. Such flows can be summarized as follows:

$$\mathbf{s}'_i = \mathbf{e}'_j \quad (\text{Downward flow}), \quad (3)$$

$$\mathbf{t}'_i = \frac{1}{n_i} \sum_{k=1}^{n_i} \mathbf{t}_k \quad (\text{Upward flow}), \quad (4)$$

where $c_j \in \mathcal{H}$ is the parent of c_i , $c_k \in \mathcal{H}$ is a child of c_i , and n_i is the number of c_i 's children. After this flow process, we use Equation (2) on \mathbf{s}'_i and \mathbf{t}'_i to calculate the new public embedding vector \mathbf{e}_i .

To reconstruct the hierarchical structure \mathcal{H} , we aim to minimize an overall distance among all nodes in \mathcal{H} . We use \mathbf{e}_i to calculate the distance between two medical codes because \mathbf{e}_i contains the information passed from c_i 's parent and children. We assume the distance should be small between two connected nodes, while large for unconnected nodes. Let $\mathcal{A} = \{(i, j) \mid c_i, c_j \in \mathcal{H}\}$ be the set of connected node pairs in \mathcal{H} , the loss function \mathcal{L}_{rec} of reconstructing the hierarchical

structure using the hyperbolic distance between two node embedding vectors is defined as:

$$\mathcal{L}_{\text{rec}} = - \sum_{(i,j) \in \mathcal{A}} \log \frac{e^{-d(\mathbf{e}_i, \mathbf{e}_j)}}{\sum_{j' \in \mathcal{N}(i) \cup \{v\}} e^{-d(\mathbf{e}_i, \mathbf{e}_{j'})}}. \quad (5)$$

Here, $\mathcal{N}(i) = \{j' \mid (c_i, c_{j'}) \notin \mathcal{A}\}$ denotes the set of non-adjacent nodes for c_i . Finally, we use \mathcal{L}_{rec} to pre-train the representation of medical codes using back-propagation and obtain the final embedding $\mathbf{E} \in \mathbb{R}^{|\mathcal{C}| \times d}$, which is the collection of \mathbf{e}_i of medical codes in the lowest level, i.e., leaf nodes. The pre-trained medical code embeddings \mathbf{E} will be further used in the self-supervised graph learning stage.

The pseudo-code of hyperbolic embedding is shown in Procedure 1. Lines 2-6 summarize the information flow, and lines 7-9 correspond to the optimization process to pre-train the embeddings using \mathcal{L}_{rec} .

Procedure 1: HyperbolicEmbedding(\mathcal{H})

Input : The hierarchical structure \mathcal{H} of medical codes
Output: Embeddings \mathbf{E} for leaf nodes of \mathcal{H}

- 1 Randomly initialize shared and local vectors
- 2 **for** $c_i \in \mathcal{H}$ **do**
- 3 $\mathbf{e}'_i \leftarrow$ combine shared and local vector $\mathbf{s}_i, \mathbf{t}_i$
- 4 $\mathbf{s}'_i, \mathbf{t}'_i \leftarrow$ Downward and upward flow
- 5 $\mathbf{e}_i \leftarrow$ combine $\mathbf{s}'_i, \mathbf{t}'_i$
- 6 **end**
- 7 **repeat**
- 8 Calculate distance by Equation (1)
- 9 Optimizing embedding vectors using \mathcal{L}_{rec}
- 10 **until** convergence
- 11 **return** $\{\mathbf{e}_i \mid c_i \text{ is a leaf node in } \mathcal{H}\}$

C. Sherbet Graph Construction

Disease complications are closely related to their co-occurrence frequencies. For example, hypertension and heart failure are often diagnosed on the same patient. Therefore, we design a directed and weighted graph \mathcal{G} to represent the sub-graph patterns of disease complications. In this graph, each vertex c_i of \mathcal{G} is a medical code in \mathcal{C} . To describe the complication of two diseases, i.e., medical codes c_i and c_j , we create directed edges between vertices c_i, c_j using the following rule: For each medical code pair (c_i, c_j) , if c_i and c_j occur once in a record V_τ of a patient u , we add two edges (i, j) and (j, i) to \mathcal{G} . Here, we create a directed graph because we think such disease relationships are asymmetric in nature, since two diseases may not have the same influence on each other. One disease c_i could be a major complication of the other disease c_j , however, the opposite might not be true. Therefore, we use directed and weighted edges to describe such dual relationships between two diseases by quantifying such influence in an adjacency matrix $\mathbf{A} \in \mathbb{R}^{|\mathcal{C}| \times |\mathcal{C}|}$, where each element \mathbf{A}_{ij} is the weight of edge (i, j) . To model the dual influence of diseases, we first define a co-occurrence matrix, $\mathbf{B} \in \mathbb{N}^{|\mathcal{C}| \times |\mathcal{C}|}$, initialized with all zeros. When calculating the values of \mathbf{B} , we increase the elements \mathbf{B}_{ij} and \mathbf{B}_{ji} by 1 for each co-occurrence pair of c_i and c_j in each admission record of all patients. Let

$q_i = \sum_{j=1}^{|\mathcal{C}|} \mathbf{B}_{ij}$ be the sum of the i -th row of \mathbf{B} , then, the weighted adjacency matrix \mathbf{A} is calculated as follows:

$$\mathbf{A}_{ij} = \begin{cases} 0 & \text{if } i = j \text{ and } q_i \neq 0, \\ 1 & \text{if } i = j \text{ and } q_i = 0, \\ \frac{\mathbf{B}_{ij}}{q_i} & \text{otherwise.} \end{cases} \quad (6)$$

Note that \mathbf{A} is typically not symmetric, which makes \mathcal{G} a weighted and directed graph. The element \mathbf{A}_{ij} measures the frequency of the disease pair (c_i, c_j) in all co-occurrence pairs of c_i . A higher frequency implies c_j appears more times along with c_i than other medical codes. Therefore, we can infer c_j has more influence on c_i , and c_j is a more common complication of c_i than other diseases.

D. Self-Supervised Graph Learning

Graph Learning Based on the key idea of constructing the disease graph \mathcal{G} , the influence of adjacent nodes on each other corresponds to the weights on their edges. Therefore, we adopt a multi-layer graph neural network (GNN) to further learn the hidden representation of medical codes, given GNN’s scalability and effective representation power. By incorporating weighted edges, GNN can scale features and pay more attention to the neighbors with higher weights. Given the initial embedding \mathbf{E} of medical codes learned from hyperbolic embedding and the weighted adjacency matrix \mathbf{A} , the hidden representation \mathbf{X} of medical codes can be calculated by a multi-layer GNN: $\mathbf{X} = \text{GNN}(\mathbf{A}, \mathbf{E})$.

More specifically, we first use the embeddings of all medical codes as inputs: $\mathbf{H}^{(0)} = \mathbf{E}$. Then, the l -th GNN layer to aggregate the features of medical codes is described as below:

$$\mathbf{H}^{(l+1)} = \text{ReLU} \left(\hat{\mathbf{A}} \mathbf{H}^{(l)} \mathbf{W}_g^{(l)} \right). \quad (7)$$

Here, $\mathbf{H}^{(l)} \in \mathbb{R}^{|\mathcal{C}| \times d^{(l)}}$ and $\mathbf{H}^{(l+1)} \in \mathbb{R}^{|\mathcal{C}| \times d^{(l+1)}}$ is the input and output of the l -th layer, respectively. $\mathbf{W}_g^{(l)} \in \mathbb{R}^{d^{(l)} \times d^{(l+1)}}$ is the weight of the l -th layer. In addition, $\hat{\mathbf{A}}$ is a normalized adjacency matrix of \mathbf{A} , which is calculated as follows:

$$\hat{\mathbf{A}}_{ij} = \frac{\tilde{\mathbf{A}}_{ij}}{\sum_{j=0}^{|\mathcal{C}|} \tilde{\mathbf{A}}_{ij}}, \quad (8)$$

$$\tilde{\mathbf{A}} = (1 - \varphi) \mathbf{A} + \varphi \mathbf{I}, \quad (9)$$

where \mathbf{I} is the identity matrix, and $0 < \varphi < 1$ is a hyper-parameter to adjust the weight of self-loops when adding \mathbf{I} to \mathbf{A} . A larger φ denotes higher importance of the center medical code when aggregating neighbor codes into this medical code. In the last GNN layer, i.e., the L -th layer, we get the output of the graph neural network. We let $\mathbf{X} = \mathbf{H}^{(L)} \in \mathbb{R}^{|\mathcal{C}| \times m}$ be the hidden representation learned by the GNN, where $m = d^{(L)}$ is the dimension of the hidden embedding in the last layer.

Multi-level attention as encoder After obtaining the hidden representation \mathbf{X} of all medical codes in \mathcal{C} , we want to use all records in the EHR data to further train the model parameters as well as the embedding matrix \mathbf{E} of medical codes. The data includes both single and multiple admission

records. For each patient u , the encoder encodes all admission records of u into a patient vector \mathbf{p} to represent u using \mathbf{X} :

$$\mathbf{p} = \text{Encoder}(V_1, V_2, \dots, V_T | \mathbf{X}). \quad (10)$$

Specifically, we apply a two-level attention mechanism:

Code-level attention: Without loss of generality, we assume an admission record V_τ of a patient u contains n medical codes. Then, the embedding \mathbf{x}_i of each medical code $c_i \in V_\tau$ can be looked up with \mathbf{X} . We adopt a global attention mechanism [30] on the medical codes in V_τ to aggregate their embeddings and calculate the admission embedding \mathbf{v}_τ for the τ -th admission:

$$\mathbf{z}_i = \tanh(\mathbf{W}_c \mathbf{x}_i) \in \mathbb{R}^a, \quad (11)$$

$$\alpha_\tau^i = \frac{\exp(\mathbf{z}_i^\top \mathbf{w}_\alpha)}{\sum_{j=1}^n \exp(\mathbf{z}_j^\top \mathbf{w}_\alpha)} \in \mathbb{R}, \quad (12)$$

$$\mathbf{v}_\tau = \sum_{i=1}^n \alpha_\tau^i \mathbf{x}_i \in \mathbb{R}^m. \quad (13)$$

Here, $\mathbf{W}_c \in \mathbb{R}^{a \times m}$ is a weight matrix, where a is the attention dimension. $\mathbf{w}_\alpha \in \mathbb{R}^a$ is the weight to calculate the attention score α_τ^i for medical code c_i in an admission. The code attention score $\alpha_\tau = [\alpha_\tau^1, \alpha_\tau^2, \dots, \alpha_\tau^n]$ measures the distribution of the medical codes in an admission. Finally, we multiply the score with x_i and calculate the weighted sum of all medical code embeddings as the admission embedding \mathbf{v}_τ .

Admission-level attention: After calculating the embedding \mathbf{v}_τ of τ -th admission of a patient, we need to learn the patient embedding using all admissions. First, we project the admission embedding \mathbf{v}_τ to the patient dimension:

$$\tilde{\mathbf{v}}_\tau = \text{LeakyReLU}(\mathbf{W}_u \mathbf{v}_\tau) \in \mathbb{R}^p. \quad (14)$$

Here, $\mathbf{W}_u \in \mathbb{R}^{p \times m}$ is a weight matrix. p is the patient dimension. We use LeakyReLU [31] as the activation function.

Similar to code-level attention, we also use the global attention for admissions to aggregate the admission embeddings and calculate the patient embedding \mathbf{p} . However, the original global attention can only measure the significance of each admission, while it cannot distinguish the contribution of each admission to the specific dimension of the output. For example, if a model predicts a set of diagnoses in the next admission, given 5 previous admissions, we aim to quantify the contribution of each admission to each predicted code. Therefore, besides the attention weight calculated by Equation (12), we also design a coefficient θ_τ to quantify such contribution.

$$\mathbf{r}_\tau = \tanh(\mathbf{W}_v \tilde{\mathbf{v}}_\tau) \in \mathbb{R}^b, \quad (15)$$

$$\beta_\tau = \frac{\exp(\mathbf{r}_\tau^\top \mathbf{w}_\beta)}{\sum_{\tau=1}^T \exp(\mathbf{r}_\tau^\top \mathbf{w}_\beta)} \in \mathbb{R}, \quad (16)$$

$$\theta_\tau = \frac{\exp(\mathbf{r}_\tau^\top \mathbf{W}_\theta)}{\sum_{\tau=1}^T \exp(\mathbf{r}_\tau^\top \mathbf{W}_\theta)} \in \mathbb{R}^p, \quad (17)$$

$$\mathbf{p} = \sum_{\tau=1}^T \beta_\tau \theta_\tau \odot \tilde{\mathbf{v}}_\tau \in \mathbb{R}^p. \quad (18)$$

Here, $\mathbf{W}_v \in \mathbb{R}^{b \times p}$ is a weight matrix and $\mathbf{w}_\beta \in \mathbb{R}^b$ is the weight to calculate the attention score $\beta_\tau \in \mathbb{R}$ for t -th

admission. The attention score $\beta = [\beta_1, \beta_2, \dots, \beta_T]$ measures the distribution within admissions. In addition, $\mathbf{W}_\theta \in \mathbb{R}^{b \times p}$ is the weight used in calculating the attention score θ_τ . The attention score $\theta = [\theta_1, \theta_2, \dots, \theta_T]$ is the distribution of \mathbf{v}_τ over each dimension of the patient embedding. Finally, we calculate the weighted sum of \mathbf{v}_τ as the patient embedding \mathbf{p} . Specifically, the weight is calculated by the multiplication of β_τ and θ_τ , and \odot the element-wise multiplication. Here, we propose Equation (18) because we want to simultaneously measure the importance of an admission compared to other admissions (β_τ), and the contribution of this admission to the output (θ_τ). We will further elaborate this idea in Section III-F, Model Interpretability.

Procedure 2 summarizes the pseudo-code of the multi-level attention encoder. Lines 2-4 calculate admission vectors using the code-level attention. Then the patient vector \mathbf{p} is computed using the admission level attention at line 5.

Procedure 2: Encoder($u, \mathcal{D}, \mathbf{X}$)

Input : A patient u , an EHR dataset \mathcal{D} , the GNN output of medical code embeddings \mathbf{X}

Output: The patient embedding vector \mathbf{p} of u

- 1 $V_1, V_2, \dots, V_T \leftarrow$ Get admission records of u from \mathcal{D}
 - 2 **for** $\tau \leftarrow 1$ to T **do**
 - 3 $\mathbf{v}_\tau \leftarrow$ Calculate the admission embedding using the code-level attention with \mathbf{X}
 - 4 **end**
 - 5 $\mathbf{p} \leftarrow$ Calculate the patient embedding using the admission-level attention
 - 6 **return** \mathbf{p}
-

Self-supervised learning To leverage all records in an EHR dataset, we need to utilize records of single-admission patients and final admission records of multiple-admission patients. Since these records lack labels regarding their next potential admissions, we focus on reconstructing historical diagnoses using the patient embedding \mathbf{p} . We conjecture that the learned patient representation will be able to reflect the historical admission records of this patient. Therefore, recovering the historical diagnoses of this patient takes advantage of the complete dataset and further optimizes the hidden representation of medical codes.

Assuming the historical diagnoses set is denoted as \mathcal{V} , we aim to decode the medical codes from \mathbf{p} into the probability distribution $\hat{\mathbf{y}}$ of predicted historical medical codes: $\hat{\mathbf{y}}_i = P(c_i \in \mathcal{V} \mid \mathbf{p})$. A naïve method is using a multilayer perceptron (MLP) to simulate the function: $\hat{\mathbf{y}} = \sigma(\text{MLP}(\mathbf{p}))$. This method directly predicts the distribution from \mathbf{p} but does not utilize the hierarchical structure of medical codes. We can make level-wise predictions by calculating the conditional probability of lower levels, once we get the probability of higher level. Therefore, we design a *hierarchy-enhanced historical prediction* task to incorporate the hierarchical structure of medical codes.

Definition 3 (Historical hierarchy of diagnoses). Given a patient u , the historical hierarchy of diagnoses in the h -th level of \mathcal{H} is defined as $\mathcal{V}^h = \{\rho_{c_i}^h \mid c_i \in \bigcup_{\tau=1}^T V_\tau\}$, where $\rho_{c_i}^h$ denotes the ancestor of c_i in h -th level, and at the leaf level, $\rho_{c_i}^H = c_i$.

Here, \mathcal{V}^h is the set of medical codes in level h that u has ever been diagnosed during u 's previous T admissions.

Definition 4 (Hierarchy-enhanced historical prediction). Given a patient u , this task is to predict the probability distribution $\hat{\mathbf{y}}^h \in \mathbb{R}^{n_h}$ of ground-truth labels in the h -th level ($h = 1, \dots, H$), where n_h is the number of medical codes in h -th level, and $n_H = |\mathcal{C}|$.

This is a multi-label classification task for each level. Given a code $c_i = \rho_{c_i}^h$ in the h -th level, according to the directed graphical model for joint probability [32], the joint probability $\hat{\mathbf{y}}_j^h = P(\rho_{c_i}^h \in \mathcal{V}^h, \rho_{c_i}^{h-1} \in \mathcal{V}^{h-1}, \dots, \rho_{c_i}^1 \in \mathcal{V}^1 \mid \mathbf{p})$ can be calculated as follows:

$$\begin{aligned} \hat{\mathbf{y}}_j^h &= P(\rho_{c_i}^h \in \mathcal{V}^h, \rho_{c_i}^{h-1} \in \mathcal{V}^{h-1}, \dots, \rho_{c_i}^1 \in \mathcal{V}^1 \mid \mathbf{p}) \\ &= P(\rho_{c_i}^1 \in \mathcal{V}^1 \mid \mathbf{p}) \prod_{k=2}^h P(\rho_{c_i}^k \in \mathcal{V}^k \mid \rho_{c_i}^{k-1} \in \mathcal{V}^{k-1}, \mathbf{p}) \\ &= \prod_{k=2}^h P(\rho_{c_i}^k \in \mathcal{V}^k \mid \rho_{c_i}^{k-1} \in \mathcal{V}^{k-1}, \mathbf{p}). \end{aligned} \quad (19)$$

Here, $P(\rho_{c_i}^1 \in \mathcal{V}^1 \mid \mathbf{p}) = 1$ because \mathcal{V}^1 only contains the root of \mathcal{H} . Then, we use a dense layer to calculate each conditional probability:

$$P(\rho_{c_i}^k \in \mathcal{V}^k \mid \rho_{c_i}^{k-1} \in \mathcal{V}^{k-1}, \mathbf{p}) = \sigma(\mathbf{w}_k \mathbf{p})_{\rho_{c_i}^k} \quad (20)$$

where $\mathbf{w}_k \in \mathbb{R}^{n_k \times p}$ decodes the patient embedding \mathbf{p} to the probability of the medical codes in the k -th level, and n_k is the number of medical codes in k -th level.

Finally, the decoder with the hierarchical prediction are defined as follows:

$$\hat{\mathbf{y}}_j^h = \text{Decoder}(\mathcal{H}, \mathbf{p}) = \prod_{k=2}^h \sigma(\mathbf{w}_k \mathbf{p})_{\rho_{c_i}^k}, \quad (21)$$

$$\mathcal{L} = \frac{1}{H-1} \sum_{h=2}^H \frac{1}{n_h} \text{CrossEntropy}(\hat{\mathbf{y}}^h, \mathbf{y}^h). \quad (22)$$

Here, \mathbf{y}^h is the ground-truth of medical codes in the h -th level. $\mathbf{y}_j^h = 1$ means $c_j = \rho_{c_i}^h \in \mathcal{V}^h$. Note that, as a self-supervised learning problem, this proxy task is not a simple input reconstruction. It predicts the hierarchy of a set of diagnoses given the admission sequence. Hence, it is different from G-BERT [12], which is a pre-training method and reconstructs the diagnoses and medicines given the same inputs.

E. Fine-tuning and Inference

After self-supervised learning, we can obtain the learned embeddings of medical codes and model parameters. For a specific task given the same format of inputs, we first calculate the patient embedding \mathbf{p} . Then, we use a fully-connected layer for the real prediction task in Definition 2. Finally, we calculate the estimated output $\hat{\mathbf{y}}'$ and the fine-tuning loss \mathcal{L}' to optimize the encoder model including the medical code embeddings and model parameters:

$$\hat{\mathbf{y}}' = g(\mathbf{W}\mathbf{p}) \in \mathbb{R}^o, \quad (23)$$

$$\mathcal{L}' = \text{Loss}(\mathbf{y}', \hat{\mathbf{y}}', \Theta), \quad (24)$$

where $\mathbf{W} \in \mathbb{R}^{o \times p}$ is the weight matrix to calculate the output and o represents the output size. g denotes the activation function. \mathbf{y}' is the ground-truth label and Θ is the set of parameters of the model. Note that \mathbf{y}', g, o , and the loss function depend on specific tasks. When optimizing the model with back-propagation, we still keep the embedding matrix and parameters learnable.

The pseudo-code of Sherbet including self-supervised learning and fine-tuning is summarized in Algorithm 1. It first pre-trains the hyperbolic embeddings of medical codes at line 1. Then the Sherbet-Graph is constructed and a graph neural network is applied at lines 2-8. The self-supervised learning framework calculates the patient vector for each patient in \mathcal{D} , predicts the historical hierarchy of diagnoses, and optimizes the model at lines 9-17. Finally, fine-tuning is executed for specific tasks at lines 18-23.

Algorithm 1: Sherbet-Optimization(\mathcal{H}, \mathcal{D})

Input : The hierarchical structure \mathcal{H} of medical codes, an EHR dataset \mathcal{D}

- 1 $\mathbf{E} \leftarrow$ HyperbolicEmbedding(\mathcal{H})
- 2 $\hat{\mathbf{A}} \leftarrow$ Construct graph \mathcal{G} and calculating normalized adjacency matrix by Equation (8)
- 3 $L \leftarrow$ Graph layer number
- 4 $\mathbf{H}^{(0)} \leftarrow \mathbf{E}$
- 5 **for** $l \leftarrow 0$ **to** $L - 1$ **do** // Graph learning
- 6 | $\mathbf{H}^{(l+1)} \leftarrow$ Aggregate $\mathbf{H}^{(l)}$ by Equation (7)
- 7 **end**
- 8 $\mathbf{X} \leftarrow \mathbf{H}^{(L)}$
- 9 **repeat** // Self-supervised learning
- 10 | $u \leftarrow$ a patient in \mathcal{D}
- 11 | $\mathbf{p} \leftarrow$ Encoder($u, \mathcal{D}, \mathbf{X}$)
- 12 | $H \leftarrow$ level number of \mathcal{H}
- 13 | **for** $h \leftarrow 2$ **to** H **do**
- 14 | | $\hat{\mathbf{y}}^h \leftarrow$ Predict level h 's labels by Equation (21)
- 15 | **end**
- 16 | Optimizing the model using \mathcal{L}
- 17 **until** convergence
- 18 **repeat** // Fine-tuning
- 19 | $u \leftarrow$ a patient in \mathcal{D} with multiple admissions
- 20 | $\mathbf{p} \leftarrow$ Encoder($u, \mathcal{D}, \mathbf{X}$)
- 21 | $\hat{\mathbf{y}}' \leftarrow$ Predict labels based on specific tasks
- 22 | Optimizing the model using \mathcal{L}'
- 23 **until** convergence

F. Model Interpretability

Another advantage of Sherbet is its ability to provide interpretable prediction results and learned representations (which is an important component in healthcare). Some existing models [3], [4] only focus on learning medical concept representations while neglecting personalized interpretability at the patient level. On the other hand, a few other models [17] are able to interpret at the patient level while lacking general interpretability for common medical knowledge. In Sherbet, we provide general interpretability by learning effective medical code representations as well as personalized interpretability by quantifying contributions of each medical code and admission for a patient.

Representation for medical codes. We use the output \mathbf{X} of GNN as the hidden representation of medical codes, since the

TABLE II
STATISTICS OF MIMIC-III AND EICU DATASETS FOR BOTH SINGLE (S) AND MULTIPLE (M) ADMISSIONS (ADM.)

Dataset	MIMIC-III		eICU	
	S	M	S	M
# patients	38,980	7,493	117,752	9,408
# adm.	38,980	19,894	117,752	20,209
Max. # adm.	1	42	1	7
Avg. # adm.	1	2.66	1	2.15
# codes	6,427	4,880	837	686
Max # codes per adm.	39	39	58	54
Avg # codes per adm.	10	13	3.47	4.40

proposed self-supervised graph learning framework helps to learn effective disease relations. We demonstrate the results of the learned representations in Section V-D.

Code-level contribution. We use the code-level attention scores $\alpha_\tau = [\alpha_\tau^1, \alpha_\tau^2, \dots, \alpha_\tau^n]$ to represent the contributions of medical codes in an admission, since α is a probability distribution of medical codes.

Admission-level contribution. Similar to the code-level contribution, we use β to represent the contribution of each admission for a prediction. Furthermore, we want to quantify the contribution of a specific admission to the output. For example, if the task is predicting all diagnoses in the next admission, we want to know the contribution of the t -th admission to each predicted medical code, i.e., $\hat{\mathbf{y}}_i$. Therefore, we define a coefficient $\delta = [\delta_1, \delta_2, \dots, \delta_T]$ to measure this contribution:

$$\delta_\tau = \beta_\tau \frac{\exp(\mathbf{W}\theta_\tau)}{\sum_{\tau=1}^T \exp(\mathbf{W}\theta_\tau)} \in \mathbb{R}^o, \quad (25)$$

where \mathbf{W} is the weight matrix in Equation (23). In this equation, firstly, $\mathbf{W}\theta_\tau$ projects the τ -th admission weight into the output dimension. Then it is multiplied by β_τ , so that we can measure the contribution from different admissions. Intuitively, δ_τ first calculates the contribution of each admission (β_τ), then it assigns this contribution to each dimension of the output ($\mathbf{W}\theta_\tau$). Together, the code-level and admission-level contributions are able to provide personalized interpretability for different patients.

IV. EXPERIMENTAL SETUP

Tasks and Evaluation Metrics We conduct our experiments on two tasks following the settings of GRAM [3]:

- *Diagnosis prediction.* This task predicts all medical codes in patients' next admission given their historical records. It is a multi-label classification task.
- *Heart failure prediction.* This task predicts whether a patient will be diagnosed with heart failure (HF) in the next admission given their historical records. It is a binary classification task.

The evaluation metrics used for diagnosis prediction are weighted F_1 score ($w-F_1$) as in Timeline [4] and top k recall ($R@k$) as in DoctorAI [1]. $w-F_1$ is the weighted sum of the F_1 score for each class, which measures an overall prediction performance on all classes. $R@k$ is the ratio of true positive

numbers in top k predictions to the total number of positive samples, which measures the prediction performance on a subset of classes.

The metrics to evaluate the HF prediction are the area under the ROC curve (AUC) and F_1 score since the HF prediction is a binary classification on imbalanced test data.

Datasets We use the MIMIC-III dataset [13] on both tasks and the eICU dataset [33] on the first task to evaluate the performance of our model. MIMIC-III contains 58,976 de-identified admission records between 2001 and 2012 from 46,520 patients. In each record, the diseases are encoded by the ICD-9-CM system. There are 6,981 medical codes in both single and multiple admissions. The eICU dataset records the patients’ admissions to intensive care units (ICU). For the eICU dataset, a patient could have multiple visits to hospitals, and in each hospital visit, there could be multiple admissions to ICU. However, there are not timestamps for hospital visits in the eICU dataset. Therefore, we regard each hospital visit as an independent patient, and each ICU admission as admission records V . In addition, we remove the diseases in eICU that cannot be found in the ICD-9-CM or ICD-10 system. Table II shows the basic statistics of single and multiple admissions in the MIMIC-III and eICU datasets.

We randomly split the EHR data with multiple admissions into training/validation/test data, which contain 6000/493/1000 patients for MIMIC-III, and 8000/408/1000 patients for eICU. The Sherbet graph and self-supervised learning are constructed and trained with single admission data and training data with multiple admissions to guarantee there is no leakage of test data in fine-tuning. We use all medical codes for self-supervised learning on both tasks. For the diagnosis prediction task, we predict medical codes appearing in multiple admissions. For the HF prediction task, there are 38.5% positive samples and 61.5% negative samples in MIMIC-III.

Comparison Methods We select the following state-of-the-art models to compare the performance with Sherbet:¹

- **MLP**: A deep neural networks consists of 3 layers, which uses multi-hot vectors for medical codes in an admission.
- **DoctorAI** [1]: An RNN-GRU model, which also uses multi-hot vectors as inputs.
- **RETAIN** [16]: A network of two RNNs with reverse time and attention methods. The inputs are multi-hot vectors for medical codes.
- **Deepr** [8]: A CNN model which uses the embedding of medical codes as inputs.
- **GRAM** [3]: An RNN model with a medical ontology graph. The inputs are medical code embeddings.
- **Dipole** [17]: A bi-directional RNN model with attention. The inputs are multi-hot vectors.
- **Timeline** [4]: An RNN model with attention, using the time duration information. The inputs are the embeddings of medical codes.
- **G-BERT*** [12]: A BERT-based model with a medical ontology graph. It first pre-trains the model on a self-prediction task and a dual-prediction task. Then fine-tunes the model

to predict the medicine. Here, we modify G-BERT* by removing the medication module and change the fine-tuning module to predict diagnoses and heart failure.

Parameter Settings for Sherbet We randomly initialize all embeddings and model parameters. The embedding sizes d, m, p for $\mathbf{E}, \mathbf{X}, \mathbf{p}$ are 128, 64, and 64, respectively. We use one graph layer where the hidden unit number is 64. The attention sizes a, b for code-level and admission-level attention are 64 and 32, respectively. The weight φ on the adjacent matrix is 0.9. In addition, for fine-tuning, we add Dropout layers [36] on each graph layer and the input of the decoder. The graph layers’ dropout rates of two tasks on MIMIC-III and diagnosis prediction on eICU are 0.2, 0.8, and 0.2, respectively. The decoder’s dropout rates are 0.02, 0.15, and 0.15, respectively. For both tasks, the activation and loss function in fine-tuning is Sigmoid and cross-entropy loss.

We use 500 epochs for pre-training hyperbolic embeddings. For self-supervised learning, we use 1000 and 300 epochs on MIMIC-III and eICU respectively, and 200 epochs for fine-tuning with a learning rate decay strategy. The initial learning rate for hyperbolic embedding is 0.01, which decays by 0.01 every 100 epochs. The initial learning rate for self-supervised learning is 0.01, which decays at the (100, 500)-th epoch by 0.1 on MIMIC-III, and decays at the (100, 250)-th epoch by 0.1 on eICU. The initial learning rate for fine-tuning is 0.01, which decays at (20, 35, 100)-th and (50, 60, 100)-th epoch for diagnosis prediction on MIMIC-III and eICU, and decays at (25, 40, 45) epochs for HF prediction on MIMIC-III. We use the Adam optimizer [37] for hyperbolic embedding and RMSProp optimizer [38] for self-supervised learning and fine-tuning. The batch sizes for hyperbolic embedding, self-supervised learning, and fine-tuning are 256, 128, and 32 respectively.

All programs are implemented using Python 3.7.4 and Tensorflow 2.3.0 with CUDA 10.1 on a machine with Intel i9-9900K CPU, 64GB memory, and Geforce RTX 2080 Ti GPU.²

Parameter Settings for Baselines The detailed parameter setting for baselines are given as follows:

- **MLP**: The hidden units for two hidden layers are 128 and 64, respectively.
- **DoctorAI**: The hidden size for the RNN layer is 128.
- **RETAIN**: The embedding size for admissions is 256. The hidden layer size for two RNN layers is 128.
- **Deepr**: The embedding size for medical codes is 100. The kernel size and filter number for an 1-D CNN layer are 3 and 128, respectively.
- **GRAM**: The embedding size for medical codes is 100. The attention size is 100. The hidden size for the RNN layer is 128.
- **Dipole**: The embedding size for admissions is 256. The concatenation-based attention size is 128. The hidden size for the RNN layer is 128.
- **Timeline**: The embedding size for medical codes is 100. The attention size is 100. The hidden size for the RNN layer is 128.

¹We do not compare with MiME [34], GCT [26], and MPVAA [35] since we do not use treatment, lab result, and demographic features in this work.

²The source code of Sherbet can be found at <https://github.com/LuChang-CS/sherbet>.

TABLE III
DIAGNOSIS PREDICTION RESULTS ON MIMIC-III AND eICU USING $w-F_1$ (%) AND $R@k$ (%).

Models	MIMIC-III				eICU			
	$w-F_1$	$R@10$	$R@20$	# Params	$w-F_1$	$R@10$	$R@20$	# Params
MLP	11.68 (0.12)	26.01 (0.04)	26.99 (0.03)	1.38M	39.45 (0.08)	63.52 (0.12)	71.59 (0.09)	0.40M
DoctorAI	12.04 (0.04)	25.69 (0.11)	27.21 (0.08)	2.53M	64.13 (0.28)	77.08 (0.32)	81.79 (0.26)	0.50M
RETAIN	18.37 (0.79)	32.12 (0.82)	32.54 (0.62)	2.90M	65.04 (1.03)	78.68 (0.92)	83.48 (1.08)	0.85M
Deepr	11.68 (0.02)	26.47 (0.02)	27.53 (0.11)	1.16M	45.89 (0.21)	67.63 (0.15)	74.01 (0.18)	0.19M
GRAM	20.78 (0.14)	34.17 (0.19)	35.46 (0.26)	1.59M	57.95 (0.05)	75.67 (0.03)	81.52 (0.03)	0.41M
Dipole	14.66 (0.20)	28.73 (0.20)	29.44 (0.20)	2.18M	58.41 (0.18)	75.66 (0.24)	81.06 (0.19)	0.56M
Timeline	16.04 (0.72)	30.73 (0.79)	32.34 (0.90)	1.23M	57.04 (1.23)	74.40 (1.17)	79.86 (0.86)	0.30M
G-BERT*	22.28 (0.25)	35.62 (0.18)	36.46 (0.15)	5.63M	63.61 (0.33)	77.63 (0.44)	80.06 (0.39)	2.62M
Sherbet	25.74 (0.04)	40.46 (0.08)	41.08 (0.08)	1.23M	64.18 (0.08)	80.05 (0.09)	84.43 (0.11)	0.17M

TABLE IV
HF PREDICTION RESULTS ON MIMIC-III USING AUC (%) AND F_1 (%)

Models	AUC	F_1	# Params
MLP	80.09 (0.06)	68.17 (0.05)	0.64M
DoctorAI	82.25 (0.02)	68.42 (0.02)	1.91M
RETAIN	82.73 (0.21)	71.12 (0.37)	1.67M
Deepr	81.29 (0.01)	68.42 (0.01)	0.53M
GRAM	82.82 (0.06)	71.43 (0.05)	0.96M
Dipole	81.66 (0.07)	70.01 (0.04)	0.92M
Timeline	80.75 (0.46)	69.81 (0.34)	0.95M
G-BERT*	83.61 (0.18)	72.37 (0.46)	2.69M
Sherbet	86.04 (0.16)	74.27 (0.07)	0.91M

TABLE V
PREDICTION RESULTS OF SHERBET VARIATIONS

Model	Diagnosis				HF	
	MIMIC-III		eICU		AUC	F_1
	$w-F_1$	$R@10$	$w-F_1$	$R@10$		
Sherbet	25.74	40.46	64.18	80.05	86.04	74.27
Sherbet _b	25.46	39.54	62.75	78.86	85.20	72.28
Sherbet _c	25.21	39.21	62.52	78.51	84.47	71.58
Sherbet _d	23.92	37.91	58.75	77.58	83.18	71.36
Sherbet _e	22.12	36.74	58.45	77.21	82.35	70.67
Sherbet _f	25.37	39.28	63.01	78.62	84.51	73.26

- **G-BERT***: The parameter settings are the same as [12]. (1) GAT part: The input embedding size is 75, the number of attention heads is 4; (2) BERT part: the hidden size is 300. The position-wise feed-forward networks include 2 hidden layers with 4 attention heads for each layer. The dimension of each hidden layer is 300.

V. EXPERIMENTAL RESULTS

A. Prediction Results

Table III shows the results of the weighted F_1 score and top k recall on the diagnosis prediction task using both datasets. We select $k = [10, 20]$ to calculate the $R@k$, because the average medical code numbers of an admission are 13 and 4.40 in MIMIC-III and eICU, respectively. In Table III, we can observe that Sherbet outperforms the baseline models in most cases. Note that, the performance on eICU is much better than MIMIC-III. This is primarily due to the fact that eICU has only 686 medical codes, while MIMIC-III has 4,880. The comparison among Sherbet, G-BERT* and GRAM indicates that self-supervised learning significantly improves the prediction results on both datasets, since they all use medical ontology information.

Table IV demonstrates the AUC and F_1 scores of the results for the HF prediction task. We use only MIMIC-III because some diseases are removed in the eICU dataset. Similar to the diagnosis prediction task, Sherbet obtains the superior performance on AUC and F_1 . In this task, compared to the best baseline model, the improvement of Sherbet is not as significant as the diagnosis prediction. We infer that the self-supervised learning is able to learn a general knowledge

representation of diseases, while HF is only one of the many diseases. On the contrary, as a multi-label classification, the diagnosis prediction task can fully utilize the representation learned by the self-supervised learning, and distinguish each type of diseases in the output.

In summary, the prediction results on diagnosis and HF prediction tasks demonstrate the superior performance of the proposed framework over state-of-the-art models.

B. Ablation Study

To study the effectiveness of each module in Sherbet, we also compare five types of Sherbet with some modules removed or replaced:

- **Sherbet_b**: Sherbet with self-supervised learning and hierarchical prediction, removing hyperbolic embedding.
- **Sherbet_c**: Sherbet with self-supervised learning, removing hyperbolic embedding and hierarchical prediction.
- **Sherbet_d**: Sherbet with hyperbolic embedding, removing self-supervised learning.
- **Sherbet_e**: Sherbet removing self-supervised learning.
- **Sherbet_f**: Sherbet with the multi-level attention encoder replaced by T-LSTM [39].

We report the results of Sherbet and Sherbet_{b~f} on two tasks in Table V. We can firstly observe that the complete Sherbet achieves the best performance among Sherbet_{b~f}, which proves the effectiveness of our proposed model. The comparison between Sherbet and Sherbet_b, and Sherbet_d and Sherbet_e shows that the hyperbolic embedding can effectively initialize the representations of medical codes. The results of Sherbet_b and Sherbet_c indicates that the hierarchical structure

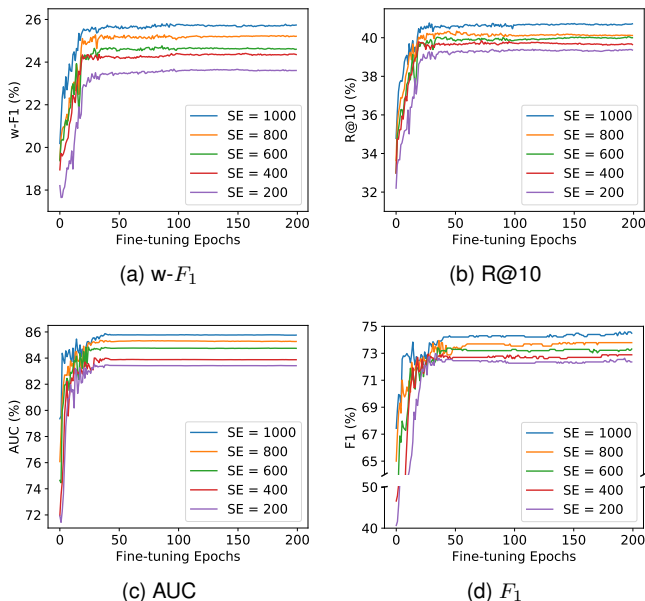


Fig. 4. The prediction results using $w-F_1$, $R@10$ on the diagnosis prediction, and AUC, F_1 on the HF prediction with five different self-supervised learning epochs (SE).

of medical codes is helpful to guide the prediction. We can also see that the performance of Sherbet_c has a large improvement over Sherbet_e, which shows the importance of self-supervised learning. However, the performance improvement of Sherbet_c over Sherbet_d on HF prediction is not as significant as the improvement over Sherbet_e. We infer that the hyperbolic embedding is also effective without self-supervised learning when the number of predicted medical codes is small. In addition, after replacing the multi-level attention with T-LSTM, the performance of Sherbet_f is not as good as Sherbet. Finally, even without self-supervised learning and hyperbolic embedding, our model still achieves top performance among baselines in Table III and IV, which shows the effectiveness of the framework.

C. Self-supervised Learning Study

To further study the effectiveness and impact of self-supervised learning, we adopt different self-supervised learning epochs (SE). On both tasks, we select five different SE as [200, 400, 600, 800, 1000] to report the variation of $w-F_1$, $R@10$ of the diagnosis prediction, and AUC and F_1 of the HF prediction on the validation data of both tasks in MIMIC-III during the fine-tuning phase.

Fig. 4 shows the validation results of the evaluation metrics of the diagnosis prediction and the HF prediction on different self-supervised learning epochs. In Fig. 4(a) and 4(b) of the diagnosis prediction results, we can see that SE has a significant influence on the fine-tuning results. Larger SE not only produces higher $w-F_1$ and $R@10$, but also speeds up the convergence. As shown in Fig. 4(c) and 4(d) of the HF prediction, the final values of AUC and F_1 are not affected too much by SE compared to the diagnosis prediction. However, lower self-supervised learning epochs still give worse

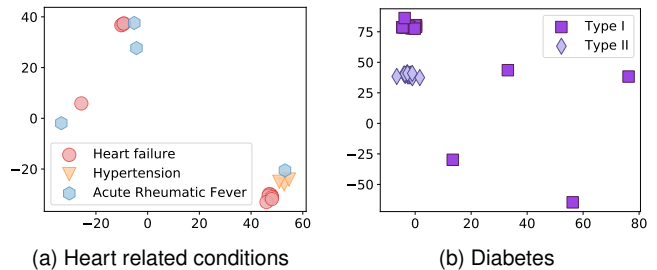


Fig. 5. Scatter plot of heart related conditions and different diabetes using t-SNE. (a) The complications between different types of heart failure, hypertension, and acute rheumatic fever, a disease that can affect the heart. (b) Diabetes type I and type II.

results. Therefore, we can further conclude that self-supervised learning on the historical hierarchy prediction task helps in improving the prediction performance on different tasks and accelerates the training of the model.

D. Case Studies for Model Interpretation

We interpret Sherbet by illustrating the representation of some typical disease complications learned by Sherbet on MIMIC-III, and visualizing the contributions introduced in Section III-F.

1) *Representation of disease complication*: In order to demonstrate if Sherbet successfully captures the disease complications, we adopt the embedding matrix \mathbf{X} , i.e. the output of the graph neural network, as the final representation learned by self-supervised learning. Then, we use t-SNE [40] to project \mathbf{X} into two dimensions. In the next step, we select 15 types of heart failure³, 3 types of essential hypertension⁴, and 7 types of acute rheumatic fever⁵ that appear in MIMIC-III and plot them in Fig. 5(a). As Fig. 5(a) shows, they are mainly grouped into three clusters. In addition, hypertension locates near one cluster of heart failure, and acute rheumatic fever locates near the three clusters of heart failure. Given that hypertension and acute rheumatic fever are two common comorbidities of heart-related diseases, they are often diagnosed in the same set of patients. It indicates that the proposed method learns similar embeddings for similar diseases or complications. Next, we select two types of diabetes⁶: type I and type II, and plot their embeddings in Fig. 5(b). As we can see in Fig. 5(b), there are no joint clusters between diabetes type I and diabetes type II. We infer that the complications of diabetes type I and diabetes type II are different to some extent. To summarize, Sherbet is able to capture the disease complications. It can also distinguish different types of diseases based on their different complications. Therefore, Sherbet can provide the general interpretability for diseases using the learned hidden representations of medical codes.

2) *Quantification of multi-level attention*: To measure the contributions both at the code-level and at the admission-level explained in Section III-F, we visualize the code-level

³www.icd9data.com/2015/Volume1/390-459/420-429/428/

⁴www.icd9data.com/2015/Volume1/390-459/401-405/401/

⁵www.icd9data.com/2015/Volume1/390-459/390-392/

⁶www.icd9data.com/2015/Volume1/240-279/249-259/250/

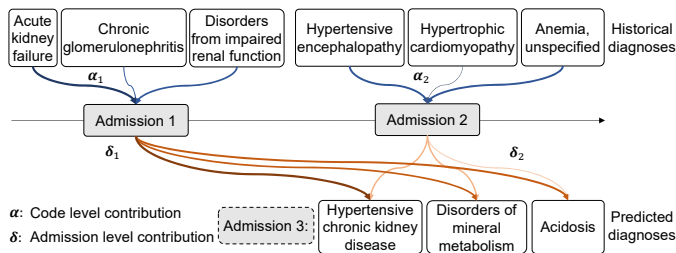


Fig. 6. Contribution of diagnoses to each admission, and admissions to each predicted diagnosis. In this case, the patient has two historical admissions. We use two admissions to predict diagnoses in the third admission.

attention distribution α in Equation (12), and coefficient δ in Equation (25) for a given patient u on the diagnosis prediction task. Fig. 6 demonstrates the historical diagnoses, the admissions, and the predicted diagnoses for a patient in rectangles. The contribution α and δ are represented by blue and red lines, respectively. The thickness and darkness of the line denote different values of α and δ . Thicker and darker lines correspond to larger values of α and δ . In this case, there are 6 diagnoses in the first admission and 10 diagnoses in the second admission, and we select 3 important diagnoses for both admissions. There are also 6 diagnoses of the third admission of this patient, i.e., ground truth diagnoses, and we show 3 correct predictions in Fig. 6.

In the first admission, the three diagnoses are all kidney-related diseases. Acute kidney failure and disorders resulting from impaired renal function mainly contribute to this admission. In the second admission, the diagnoses are brain, heart, and blood related, respectively. Hypertensive encephalopathy and Anemia mainly contribute to this admission. In the third admission, we can see that the correct predictions are all metabolic diseases and kidney disease. Therefore, Sherbet predicts that the first admission contributes more than the second admission. More specifically, the first admission contributes mainly to hypertensive chronic kidney disease because the patient is diagnosed with acute kidney failure in the first admission. We can also infer that kidney problems of this patient mainly cause the metabolic diseases in the third admission. For the second admission, we can discover that it mainly contributes to hypertensive chronic kidney disease. We believe that it is due to the fact this patient has hypertensive encephalopathy. High blood pressure causing hypertensive encephalopathy also causes hypertensive chronic kidney disease in this admission. Besides, anemia in the second admission could also be a cause of the metabolic diseases in the third admission. In summary, Sherbet provides quantitative personalized interpretability using the contributions α and δ learned from patients' historical diagnoses and admissions.

VI. CONCLUSION

In this paper, we propose Sherbet, a *self-supervised graph learning framework with hyperbolic embeddings for medical codes to predict temporal health events*. We first take advantage of the hierarchical structure of medical codes to pre-train a hyperbolic embedding. Then, we adopt a graph neural network with a weighted and directed graph of medical

codes to learn disease complications in EHR data. With the code-level and specially-designed admission-level attention mechanism, Sherbet is able to simultaneously provide general interpretability for medical concepts and personalized interpretability for patients. In addition, we also design a self-supervised proxy task to predict the historical hierarchy of diagnoses in patients' admission records by further utilizing the hierarchical structure of medical codes. This task is able to leverage more data by incorporating single admission records and the final admissions of multiple admission records. Our experimental results show the improved performance of Sherbet over state-of-the-art methods. We also illustrate the general and personalized interpretability of Sherbet by case studies. One shortcoming of Sherbet is that it only utilizes disease codes in patients' admission records. In the future, we will explore the relationships of more features such as procedures, medicines, and lab results.

REFERENCES

- [1] E. Choi, M. T. Bahadori, A. Schuetz, W. F. Stewart, and J. Sun, "Doctor ai: Predicting clinical events via recurrent neural networks," in *Machine Learning for Healthcare Conference*, 2016, pp. 301–318.
- [2] N. Zheng, S. Du, J. Wang, H. Zhang, W. Cui, Z. Kang, T. Yang, B. Lou, Y. Chi, H. Long *et al.*, "Predicting covid-19 in china using hybrid ai model," *IEEE Transactions on Cybernetics*, 2020.
- [3] E. Choi, M. T. Bahadori, L. Song, W. F. Stewart, and J. Sun, "Gram: graph-based attention model for healthcare representation learning," in *Proceedings of the 23rd ACM SIGKDD International Conference on Knowledge Discovery & Data Mining*, 2017, pp. 787–795.
- [4] T. Bai, S. Zhang, B. L. Egleston, and S. Vucetic, "Interpretable representation learning for healthcare via capturing disease progression through time," in *Proceedings of the 24th ACM SIGKDD International Conference on Knowledge Discovery & Data Mining*, 2018, pp. 43–51.
- [5] D. Nguyen, W. Luo, S. Venkatesh, and D. Phung, "Effective identification of similar patients through sequential matching over icd code embedding," *Journal of medical systems*, vol. 42, no. 5, p. 94, 2018.
- [6] B. Yang, M. Ye, Q. Tan, and P. C. Yuen, "Cross-domain missingness-aware time-series adaptation with similarity distillation in medical applications," *IEEE Transactions on Cybernetics*, 2020.
- [7] S. Darabi, M. Kachuee, S. Fazeli, and M. Sarrafzadeh, "Taper: Time-aware patient EHR representation," *IEEE Journal of Biomedical and Health Informatics*, 2020.
- [8] P. Nguyen, T. Tran, N. Wickramasinghe, and S. Venkatesh, "Deepr: A convolutional net for medical records," *IEEE Journal of Biomedical and Health Informatics*, vol. 21, no. 1, pp. 22–30, Jan 2017.
- [9] Z. Huang, W. Dong, H. Duan, and J. Liu, "A regularized deep learning approach for clinical risk prediction of acute coronary syndrome using electronic health records," *IEEE Transactions on Biomedical Engineering*, vol. 65, no. 5, pp. 956–968, 2017.
- [10] Z. Che, Y. Cheng, S. Zhai, Z. Sun, and Y. Liu, "Boosting deep learning risk prediction with generative adversarial networks for electronic health records," in *2017 IEEE International Conference on Data Mining (ICDM)*. IEEE, 2017, pp. 787–792.
- [11] L. Yao, Y. Zhang, B. Wei, W. Zhang, and Z. Jin, "A topic modeling approach for traditional chinese medicine prescriptions," *IEEE Transactions on Knowledge and Data Engineering*, vol. 30, no. 6, pp. 1007–1021, 2018.
- [12] J. Shang, T. Ma, C. Xiao, and J. Sun, "Pre-training of graph augmented transformers for medication recommendation," in *Proceedings of the Twenty-Eighth International Joint Conference on Artificial Intelligence, IJCAI-19*. ijcai.org, 2019, pp. 5953–5959.
- [13] A. E. Johnson, T. J. Pollard, L. Shen, H. L. Li-wei, M. Feng, M. Ghassemi, B. Moody, P. Szolovits, L. A. Celi, and R. G. Mark, "Mimic-iii, a freely accessible critical care database," *Scientific data*, vol. 3, p. 160035, 2016.
- [14] CDC, "Icd-9-cm - international classification of diseases, ninth revision, clinical modification," Nov 2015, accessed: 2020-05-10. [Online]. Available: <https://www.cdc.gov/nchs/icd/icd9cm.htm>
- [15] F. H. Messerli, S. F. Rimoldi, and S. Bangalore, "The transition from hypertension to heart failure: contemporary update," *JACC: Heart Failure*, vol. 5, no. 8, pp. 543–551, 2017.

- [16] E. Choi, M. T. Bahadori, J. Sun, J. Kulas, A. Schuetz, and W. Stewart, "Retain: An interpretable predictive model for healthcare using reverse time attention mechanism," in *Advances in Neural Information Processing Systems*, 2016, pp. 3504–3512.
- [17] F. Ma, R. Chitta, J. Zhou, Q. You, T. Sun, and J. Gao, "Dipole: Diagnosis prediction in healthcare via attention-based bidirectional recurrent neural networks," in *Proceedings of the 23rd ACM SIGKDD international conference on knowledge discovery & data mining*, 2017, pp. 1903–1911.
- [18] K. Cho, B. van Merriënboer, C. Gulcehre, D. Bahdanau, F. Bougares, H. Schwenk, and Y. Bengio, "Learning phrase representations using rnn encoder-decoder for statistical machine translation," in *Proceedings of the 2014 conference on empirical methods in natural language processing (EMNLP)*, 2014, pp. 1724–1734.
- [19] L. Jing and Y. Tian, "Self-supervised visual feature learning with deep neural networks: A survey," *IEEE Transactions on Pattern Analysis and Machine Intelligence*, 2020.
- [20] S. Gidaris, P. Singh, and N. Komodakis, "Unsupervised representation learning by predicting image rotations," in *ICLR 2018*, 2018.
- [21] L. Chen, P. Bentley, K. Mori, K. Misawa, M. Fujiwara, and D. Rueckert, "Self-supervised learning for medical image analysis using image context restoration," *Medical image analysis*, vol. 58, p. 101539, 2019.
- [22] A. Vaswani, N. Shazeer, N. Parmar, J. Uszkoreit, L. Jones, A. N. Gomez, L. Kaiser, and I. Polosukhin, "Attention is all you need," in *Advances in neural information processing systems*, 2017, pp. 5998–6008.
- [23] J. Devlin, M.-W. Chang, K. Lee, and K. Toutanova, "BERT: Pre-training of deep bidirectional transformers for language understanding," in *Proceedings of the 2019 Conference of the North American Chapter of the Association for Computational Linguistics: Human Language Technologies, Volume 1 (Long and Short Papers)*. Association for Computational Linguistics, Jun. 2019, pp. 4171–4186.
- [24] J. Pennington, R. Socher, and C. D. Manning, "Glove: Global vectors for word representation," in *Proceedings of the 2014 conference on empirical methods in natural language processing (EMNLP)*, 2014, pp. 1532–1543.
- [25] T. N. Kipf and M. Welling, "Semi-Supervised Classification with Graph Convolutional Networks," in *Proceedings of the 5th International Conference on Learning Representations*, 2017.
- [26] E. Choi, Z. Xu, Y. Li, M. W. Dusenberry, G. Flores, Y. Xue, and A. M. Dai, "Learning the graphical structure of electronic health records with graph convolutional transformer," in *Proceedings of the 34th Conference on Association for the Advancement of Artificial Intelligence*, 2020.
- [27] CDC, "Icd-10 - international classification of diseases, tenth revision," Feb 2020, accessed: 2020-05-10. [Online]. Available: <https://www.cdc.gov/nchs/icd/icd10cm.htm>
- [28] M. Nickel and D. Kiela, "Poincaré embeddings for learning hierarchical representations," in *Advances in neural information processing systems*, 2017, pp. 6338–6347.
- [29] B. Dhingra, C. Shallue, M. Norouzi, A. Dai, and G. Dahl, "Embedding text in hyperbolic spaces," in *Proceedings of the Twelfth Workshop on Graph-Based Methods for Natural Language Processing (TextGraphs-12)*, 2018, pp. 59–69.
- [30] T. Luong, H. Pham, and C. D. Manning, "Effective approaches to attention-based neural machine translation," in *Proceedings of the 2015 Conference on Empirical Methods in Natural Language Processing*. Lisbon, Portugal: Association for Computational Linguistics, Sep. 2015, pp. 1412–1421.
- [31] B. Xu, N. Wang, T. Chen, and M. Li, "Empirical evaluation of rectified activations in convolutional network," *arXiv preprint arXiv:1505.00853*, 2015.
- [32] C. M. Bishop, *Pattern recognition and machine learning*. Springer, 2006, pp. 359–361.
- [33] T. J. Pollard, A. E. Johnson, J. D. Raffa, L. A. Celi, R. G. Mark, and O. Badawi, "The eicu collaborative research database, a freely available multi-center database for critical care research," *Scientific data*, vol. 5, p. 180178, 2018.
- [34] E. Choi, C. Xiao, W. Stewart, and J. Sun, "Mime: Multilevel medical embedding of electronic health records for predictive healthcare," in *Advances in neural information processing systems*, 2018, pp. 4547–4557.
- [35] S. Chowdhury, C. Zhang, P. S. Yu, and Y. Luo, "Mixed pooling multi-view attention autoencoder for representation learning in healthcare," *arXiv preprint arXiv:1910.06456*, 2019.
- [36] N. Srivastava, G. Hinton, A. Krizhevsky, I. Sutskever, and R. Salakhutdinov, "Dropout: a simple way to prevent neural networks from overfitting," *The journal of machine learning research*, vol. 15, no. 1, pp. 1929–1958, 2014.
- [37] D. P. Kingma and J. Ba, "Adam: A method for stochastic optimization," in *3rd International Conference on Learning Representations, ICLR 2015, San Diego, CA, USA, May 7-9, 2015, Conference Track Proceedings*, Y. Bengio and Y. LeCun, Eds., 2015.
- [38] G. Hinton, N. Srivastava, and K. Swersky, "Neural networks for machine learning lecture 6a overview of mini-batch gradient descent," *Cited on*, vol. 14, no. 8, 2012.
- [39] I. M. Baytas, C. Xiao, X. Zhang, F. Wang, A. K. Jain, and J. Zhou, "Patient subtyping via time-aware lstm networks," in *Proceedings of the 23rd ACM SIGKDD international conference on knowledge discovery & data mining*, 2017, pp. 65–74.
- [40] L. v. d. Maaten and G. Hinton, "Visualizing data using t-sne," *Journal of machine learning research*, vol. 9, no. Nov, pp. 2579–2605, 2008.